AD-A102 324 AERONAUTICAL RESEARCH LABS MELBOURNE (AUSTRALIA) F/G 20/4
TURBULENT BOUNDARY LAYER FLOW THROUGH A GAP IN A WALL-MOUNTED R--ETC(U)
SEP 80 W H SCHOFIELD, D S BARBER, E LOGAN
UNCLASSIFIED ARL/MECH-ENG NOTE 384 NL

1 of 1
AD
A102324

END
DATE
FILMED
8 81
DTIC

ARL-MECH-ENG-NOTE-384 ✓

AR-002-232

LEVEL II

(12)

AD A102324

DEPARTMENT OF DEFENCE

DEFENCE SCIENCE AND TECHNOLOGY ORGANISATION

AERONAUTICAL RESEARCH LABORATORIES

MELBOURNE, VICTORIA

DTIC
ELECTE
AUG 0 3 1981
S E D

MECHANICAL ENGINEERING NOTE 384

TURBULENT BOUNDARY LAYER FLOW THROUGH A GAP IN A WALL-MOUNTED ROUGHNESS ELEMENT

by

W. H. SCHOFIELD Aeronautical Research Laboratories
D. S. BARBER United States Army Corps, West Point
E. LOGAN Arizona State University

Approved for Public Release.

THE UNITED STATES NATIONAL TECHNICAL INFORMATION SERVICE IS AUTHORISED TO REPRODUCE AND SELL THIS REPORT

DTIC FILE COPY

© COMMONWEALTH OF AUSTRALIA 1980

COPY No 22

SEPTEMBER 1980

81 8 03 012

AR-002-232

DEPARTMENT OF DEFENCE
DEFENCE SCIENCE AND TECHNOLOGY ORGANISATION
AERONAUTICAL RESEARCH LABORATORIES

MECHANICAL ENGINEERING NOTE 384

TURBULENT BOUNDARY LAYER FLOW THROUGH A GAP IN A WALL-MOUNTED ROUGHNESS ELEMENT

by

W. H. SCHOFIELD Aeronautical Research Laboratories
D. S. BARBER United States Army Corps, West Point
E. LOGAN Arizona State University

SUMMARY

The development of a turbulent boundary layer flow through a gap in an isolated wall-mounted roughness element has been studied experimentally. Two flow regions were distinguished downstream of the gap; a distortion region followed by a readjustment region. In the distortion region two counteracting distortion mechanisms were identified, the relative importance of which depended on gap size. Thus flows downstream of large gaps were found to differ significantly from those through small gaps. After distortion the layer readjusts itself and approaches equilibrium conditions of an undisturbed zero pressure gradient layer. The readjustment starts near the wall with the turbulence adjustment preceding the mean flow adjustment. The growth of the internal layer for flow through six different gap sizes can be described by a single function if internal layer height and distance from the gap are non-dimensionalized with the local wall length scale. Well downstream of the gap it is shown that all six flows are similar and are approaching equilibrium conditions in a similar manner.

POSTAL ADDRESS: Chief Superintendent, Aeronautical Research Laboratories, Box 4331, P.O., Melbourne, Victoria, 3001, Australia.

DOCUMENT CONTROL DATA SHEET

Security classification of this page: Unclassified

1. Document Numbers
   (a) AR Number:
   AR-002-232
   (b) Document Series and Number:
   Mechanical Engineering Note 384
   (c) Report Number:
   ARL-Mech-Eng-Note-384

2. Security Classification
   (a) Complete document:
   Unclassified
   (b) Title in isolation:
   Unclassified
   (c) Summary in isolation:
   Unclassified

3. Title: TURBULENT BOUNDARY LAYER FLOW THROUGH A GAP IN A WALL-MOUNTED ROUGHNESS ELEMENT

4. Personal Author(s):
   Schofield, W. H.*
   Barber, D. S.†
   Logan, E.‡

5. Document Date:
   September, 1980

6. Type of Report and Period Covered:

7. Corporate Author(s):
   * Aeronautical Research Laboratories
   † Department of Mechanics, United States Army Corps, West Point
   ‡ Department of Mechanical Engineering, Arizona State University

8. Reference Numbers
   (a) Task:
   DST 80/135
   (b) Sponsoring Agency:
   DST

9. Cost Code:
   42 7401

10. Imprint:
    Aeronautical Research Laboratories, Melbourne

11. Computer Program(s)
    (Title(s) and language(s)):

12. Release Limitations (of the document): Approved for Public Release

12.0 Overseas:	N.O.		P.R.	1	A		B		C		D		E	

13. Announcement Limitations (of the information on this page): No Limitations

14. Descriptors:
    Turbulent Boundary Layers
    Turbulence
    Surface Roughness
    Boundary Layer Flow

15. Cosati Codes:
    2004

16. *ABSTRACT*

The development of a turbulent boundary layer flow through a gap in an isolated wall-mounted roughness element has been studied experimentally. Two flow regions were distinguished downstream of the gap; a distortion region followed by a readjustment region. In the distortion region two counteracting distortion mechanisms were identified, the relative importance of which depended on gap size. Thus flows downstream of large gaps were found to differ significantly from those through small gaps. After distortion the layer readjusts itself and approaches equilibrium conditions of an undisturbed zero pressure gradient layer. The readjustment starts near the wall with the turbulence adjustment preceding the mean flow adjustment. The growth of the internal layer for flow through six different gap sizes can be described by a single function if internal layer height and distance from the gap are non-dimensionalized with the local wall length scale. Well downstream of the gap it is shown that all six flows are similar and are approaching equilibrium conditions in a similar manner.

CONTENTS

	Page No.
NOTATION	
1. INTRODUCTION	1
2. EXPERIMENT	2
3. RESULTS	2
3.1 Flow Description	2
3.2 Distortion Region	2
3.3 Readjustment Region	3
3.4 Mean Flow Parameters	5
3.5 Turbulent Flow	6
4. CONCLUSIONS	6
REFERENCES	
FIGURES	
DISTRIBUTION	

Accession For
NTIS GRA&I ☒
DTIC TAB ☐
Unannounced ☐
Justification
By
Distribution/
Availability Codes
Dist | Avail and/or Special
A

NOTATION

A	Constant in logarithmic law of the wall (5.1)
c_f'	Local skin friction coefficient ($\tau_0/\frac{1}{2}\rho u_1^2$)
c_{f0}'	Skin friction coefficient of undisturbed layer
D	Gap width
G	Clauser's profile shape factor
H	Height of roughness element (8·38 mm)
u	Mean velocity in X direction
$\sqrt{u'^2}$	Longitudinal turbulence intensity
$\sqrt{u_m'^2}$	Maximum value of $\sqrt{u'^2}$
u_τ	Friction velocity ($\sqrt{\tau_0/\rho}$)
$u_{\tau 0}$	Friction velocity of undisturbed layer
U_1	Free stream velocity in X direction
x	Distance in the main flow direction
y	Vertical distance from wall
y_m'	Value of y at $\sqrt{u_m'^2}$
z	Local wall length scale
δ	Boundary layer total thickness
δ_1	Height of internal layer
κ	von Kárman constant (0·41)
ν	Kinematic viscosity of fluid
ρ	density of fluid
τ_0	Wall shear stress

1. INTRODUCTION

There has been considerable work on the response of turbulent boundary layers to various perturbations, including changes in wall roughness and pressure gradients, changes in wall suction and injection and to obstacles in the flow. Tani[20] and Schofield[16] have reviewed this work which has both theoretical and practical applications. The theoretical interest comes from Clauser's[7] proposal that these experiments offer the possibility of understanding the internal turbulent exchange mechanisms in the boundary layer by observing the response of a layer to a step or pulse input in one of its boundary conditions. Practical interest in the experiments arises from the need to predict engineering flows involving these perturbations, for example in the fields of heat transfer, aerodynamics of jet engines, meteorology and wind loads on buildings.

The present work considers flow of a turbulent boundary layer over and through a gap in a surface-mounted roughness element, which has practical significance for example, in describing the effects of buildings and other obstructions on wind gradients and turbulence levels near V/STOL aircraft landing zones. Data on such flows have not been previously reported, but there has been work on isolated surface roughness elements without gaps. Mueller and Robertson[11] studied a flat plate flow over a wedge-shaped element the height of which was of the same order as the boundary layer thickness, and measured mean and fluctuating velocity profiles up to 40 element thicknesses downstream of the element. Reattachment of the flow separation caused by the element, defined as the position where $c_f' = 0$, occurred at seven element heights downstream of the element, after which the skin friction was found to increase rapidly to its undisturbed value. The mean and fluctuating velocity profiles were judged to have returned to their undisturbed forms at a distance of 40 element heights downstream of the element. Oka and Kostic[12] performed a similar study using a square roughness element on the floor of a rectangular channel, in which reattachment was again found to be located at seven element heights downstream of the element. Turbulence intensity profiles after reattachment showed a large maximum that decreased in magnitude and moved away from the wall with distance downstream. However, these maximum values at 18 element heights downstream of the element, were still considerably larger than values in an undisturbed layer. Similar results were reported by Counihan, Hunt and Jackson[5] who also used a square cross-section element. These authors presented an eddy viscosity theory that adequately described the mean flow profiles but gave poor predictions for the shear stress and turbulence intensity profiles. Results by Sami and Liu[15] suggest that the distance to reattachment behind an element whose height is the same as the boundary layer, depends on the Reynolds number. However, their reattachment lengths were much larger (12 to 14 element heights) than those given in other papers. Phataraphruk and Logan[14] found that the reattachment length behind a single roughness element in a smooth pipe depended on the height to width ratio of the roughness element, which may explain the different reattachment lengths reported by authors for flows behind thin two-dimensional fences (Petryk and Brundrett,[13] 17 fence heights; Good and Joubert,[8] 12–14 fence heights).

Some measurements in flows with no gap were included in the present study. Not only does this two-dimensional element case represent a limit for the experiments with a gap but by comparison with the results of previous work these tests gave confidence in the results for flows through gaps.

Of less relevance to the present study is the considerable amount of work which has been done on flow around isolated three-dimensional elements, such as measurements around a surface-mounted cube by Castro and Robins,[4] around model buildings by Sharan,[19] around a right cylinder by Hornung and Joubert[9] and around a surface-mounted aerofoil by Brown.[3] These flows all generate horseshoe vortices around the front of the models that shed from both sides of the model and decay fairly rapidly with distance downstream. The relevance of these studies to the present work is that in flow through a gap, vortices are shed from each side

of the gap and have a significant influence on flow development in the region immediately downstream of the gap.

2. EXPERIMENT

A two-dimensional turbulent boundary layer was generated and its (centreline) development observed through a gap in a wall-mounted roughness element as shown schematically in Figure 1. The element was square in cross-section (8·38 mm by 8·38 mm) and the centreline gap width was set at six different values ranging from 4·19 mm to 83·8 mm (i.e. 0·5H to 10·0H). The experimental flow was generated on the floor of a suction wind tunnel 7·32 m long and 0·56 m wide. The flexible roof of the wind tunnel was adjusted to give a zero pressure gradient flow over the length of the wind tunnel. Air for the tunnel was firstly filtered and then entered a honeycomb flow straightener. 150 mm downstream of the flow straightener the boundary layer was tripped by a 12·7 mm quarter round rod and then further thickened by 0·6 m of rough sand paper fixed to the floor. A smooth wall boundary layer was allowed to develop over a length of 4 m upstream of the roughness element under study, leaving 2·4 m of tunnel floor for observation of the boundary layer's response to the element. The Reynolds number, based on the development length of the flow at the element, was $2{\cdot}2 \times 10^6$, which was held constant for all tests. The total boundary layer thickness immediately before the element was 77 mm ($\simeq 9H$).

Pitot tubes and hot wire anemometer probes were mounted on a traversing mechanism above the roof of the tunnel, the probes entering the flow through slots in the roof. The traversing mechanism could be moved only along the tunnel centreline and hence only profiles along the centreline of the flow were recorded.

As a test of the flow and the measuring system, mean velocity and longitudinal turbulence intensity profiles were measured in an empty tunnel. These profiles were compared with zero pressure gradient profiles by Wieghardt and Tillmann[22] and Klebanoff and Diehl,[10] and gave satisfactory agreement.

3. RESULTS

3.1 Flow Description

As only centreline profiles were measured in this work the following description of the flow is rather speculative, although its major features will be fairly uncontroversial at least in qualitative terms.

Three regions can be distinguished in the flow which is shown schematically in Figure 1. The first region is well upstream of the element, where there is an undisturbed zero pressure gradient boundary layer. In the second flow region the layer flows through the gap and is distorted by it. The distortion starts before the gap and continues downstream of it where three-dimensional separations generated at each gap edge bow outwards towards the flow centreline. Thus maximum distortion is produced at a position a little downstream of the element, after which the distortion rapidly decreases and the gap edge separations join up with the separations caused by flow over the roughness element (see Fig. 1). Results suggest that most of the distortion has taken place at the longitudinal position where the separation bubble formed by flow over the roughness element closes. Downstream of this position is the third region in which the layer readjusts itself and approaches the original zero pressure gradient form which is its final equilibrium condition.

3.2 Distortion Region

Distortion of the centreline flow through the gap is caused by flow adjacent to the centreline funnelling through the gap. Here the effective lateral boundaries to the flow are formed by separated regions shedding from the gap edges, almost certainly involving counter-rotating helical vortices on each side of the centreline flow. This flow picture can explain the different behaviour of the centreline flow for large and small gap widths. Flow through the large gaps is well removed

from the gap edges and is little affected by the gap edge separations. Thus the flow funnels through the gap, increasing the mean velocity of the centreline flow and decreasing the longitudinal turbulence intensity as in a conventional nozzle. On the other hand the centreline flow through a small gap is affected by the gap edge separations which in this case occupy a significant proportion of the flow area of the gap. At the smallest gap settings considered here the gap edge separation vortices dominate the gap flow, the centreline flow is brought nearly to separation and much of the "through gap" flow is diverted up and over the gap, increasing mean flow velocities at distances greater than the element height. The gap edge separations adjacent to the centreline flow increase its turbulence level near the wall. Data supporting this flow picture are presented in Figure 2 where a series of profiles for a small gap ($D/H = 1{\cdot}0$) and for a large gap ($D/H = 5{\cdot}0$) are compared with the (upstream) undisturbed boundary layer profiles. In the distortion regime ($0 < x/H < 10$) the small gap profiles show a reduction in mean velocity near the wall and the corresponding profiles of longitudinal turbulence ($\sqrt{\overline{u'^2}}/u_{\tau 0}$) show a large increase near the wall. Note that both these series of profiles show maximum distortions at about four to six element heights downstream of the gap. This is due to the bowing out of the separation boundaries downstream of the gap.

The profiles for the large gap show the opposite behaviour. In the distortion regime the gap edge separations are well removed from the centreline and thus mean flow velocities are increased (relative to the undisturbed profile) and longitudinal turbulence intensities decreased. Note that in this case maximum distortion occurs in profiles nearest the gap† as it is the actual gap not the downstream separation boundaries that is causing the majority of the centreline distortion.

In both cases the outer portions ($y/H > 2$) of the profiles at the end of distortion ($x/H \simeq 10$) are again coincident with the undisturbed upstream profiles. This is fortunate as it aids the analysis of the layer's readjustment that is discussed in the next section.

The existence of vortices shed from the gap is supported by centreline profiles taken in the smallest gap considered ($D/H = 0{\cdot}5$). The wall regions of mean and fluctuating velocity profiles at $x/H = 0$ are shown in Figure 3. Corresponding positions in the two profiles (i.e. the same values of y/H) are marked by circled numbers at salient profile points. Figure 3*a* shows the mean profile plotted on Clauser's[6] semilogarithmic coordinates, u/U_1 versus $\log_{10} y(U_1/\nu)$. For a normal two-dimensional boundary layer this mean flow profile should show a linear distribution up to about $0{\cdot}15\delta$. However, in this case the profile shows pronounced sinuosity. The peaks and valleys of this sinuosity are closely related to sinuosity in the longitudinal turbulence intensity profile (Fig. 3*b*). The sinuosities can be followed in downstream profiles (for this gap setting) but show a rapid decay. These data give good support to the postulate of significant gap edge separations and their associated vortices affecting the centreline flow at small gap settings.

3.3 Readjustment Region

The readjustment of the centreline flow towards velocity distributions of an undisturbed zero pressure gradient layer start at about $x/H = 10$ for all gap settings. At this position distortion of the profiles by the gap is small and rapidly decaying.‡ Downstream of $x/H = 10$ the dominant feature of the flow is readjustment, which under these conditions is in many ways similar to the adjustment of a boundary layer to a new wall roughness after a rough to smooth step change in surface roughness as studied by Antonia and Luxton.[1] The "new" flow condition in the present case is the cessation of flow distorting forces rather than the cessation of a rough wall. It is well established (Tani;[20] Schofield;[16] Townsend[21]) that flow modification occurs outwards from the wall in all readjusting layers as the scale of turbulence near the wall is small, short lived and hence can make the most rapid adjustment to the new flow conditions. Further out from the wall, as well as small eddies there exist large eddies, which contain most of the

† In Figure 2 this is the profile at $x/H = 2$. Earlier profiles at $x/H = 1$, not shown in Figure 2, have slightly more distortion.

‡ This can be seen to a limited extent in Figure 2 but better evidence is presented later in connection with Figure 7.

turbulent energy, have longer lifetimes and travel downstream faster than wall eddies because they exist in regions of higher mean velocity (Townsend[21]). For these reasons the readjustment process proceeds ever more slowly as flow modification works its way outwards through the layer, and complete attainment of the final equilibrium profile appears to take a very long development distance.†

To find the height of modified flow (usually termed the height of the internal layer) δ_i, the readjusting profile is compared with the profile the layer would have had if the perturbation had not been applied to the layer (see Schofield[16,17]). In the present case the unperturbed profile is simply that of a zero pressure gradient layer and this is compared with the actual profiles in Figure 2. The rates of adjustment of various flow parameters (such as mean velocity, fluctuating velocities, turbulent shear stress) are not necessarily the same. However, as all workers in this field have measured mean velocities it is usual to determine the δ_i associated with mean velocity adjustment. Thus the height of the internal layer δ_i is defined as the distance from the wall that the actual mean velocity profile merges with the unperturbed profile, as shown in Figure 2. It can be seen that modification of the longitudinal turbulence intensity profiles precedes modification of the mean velocity for both small and large gap cases. This result applied to all six cases studied in this work.

Many authors have expressed the variation of internal layer height with distance from the perturbation in a straight dimensional form; e.g. $\delta_i \propto x^{0\cdot43}$ by Antonia and Luxton[1] for a rough to smooth wall step. Such dimensional relations may not be useful for other flows with different boundary conditions, geometries or Reynolds numbers. Schofield[17,18] has shown that non-dimensionalizing the results with the local wall length scale (z) introduced by Townsend,[21] collapses data from a very wide variety of flows over a step change in roughness onto a single curve. The wall length scale for smooth wall flow is related to the wall shear and its definition is derived from the logarithmic law of the wall which applies to the inner regions of most two-dimensional turbulent boundary layers. It can be written

$$u/u_\tau = (1/\kappa)\log_e y(u_\tau/\nu) + A \tag{1}$$

and the local wall length scale (z) is defined by rewriting it as

$$u/u_\tau = (1/\kappa)\log_e y/z \tag{2}$$

which by comparison gives

$$z = \nu/(u_\tau \exp(\kappa A))\ ‡ \tag{3}$$

Using the local value of z for each profile the variation of the non-dimensional internal layer height (δ_i/z) is compared with the non-dimensional distance from the gap (x/z) in Figure 4. It is seen that the data expressed in this form are similar, although a systematic variation with gap size can be discerned. This systematic variation could be attributable to a continuing influence of the pulse perturbation that varies with gap size. However, all the data collapse onto a single curve with little scatter as shown by the last graph in Figure 4.

Townsend's analysis considered thick zero pressure gradient flow over a small step change in roughness and gave the following relation for the internal layer height

$$(\delta_i/z)(\log_e(\delta_i/z) - 1) = 2\kappa^2(x/z). \tag{4}$$

Scholfied[17,18] showed that this equation gave quite good descriptions for flow over a wide range of step changes in roughness under all types of flow conditions, many of which were very different from those of the Townsend analysis. Equation (4) has been plotted in Figure 4 and appears to give a useful description of the internal layer growth for all six flows even though the present perturbation was of a different kind from that analysed by Townsend.

Figure 5 compares mean velocity and longitudinal turbulence intensity profiles at the last measuring station ($x/H = 224$) for all gap sizes. The mean profiles for all six cases are closely

† This is a common conclusion of Bradshaw and Wong,[2] Townsend[21] and Schofield[16,17,18] and is further demonstrated later in this paper.

‡ Values of u_τ were derived by the Clauser[6] method which is discussed later in this paper.

similar while the turbulence intensity profiles are less so. The two sets of profiles for the previous station ($x/H = 112$) are also similar but the degree of similarity is less marked. Thus it appears that during the readjustment process these six layers have "forgotten" the difference in their distortion histories and tend to common velocity distributions as they approach their final equilibrium form. Figure 5 also shows that both mean and fluctuating flows have, by $x/H = 224$, returned to their equilibrium distributions in the region immediately adjacent to the wall. However, both profiles still have considerable adjustment to make before they are identical to the undisturbed zero pressure gradient profiles. Thus these results do not agree with the conclusion of Mueller and Robertson[11] that the flow (for the zero gap case) returns to undisturbed conditions at 40 element heights downstream of the element. The present results are consistent with Bradshaw and Wong's[2] conclusion that full readjustment takes hundreds of boundary layer lengths downstream of an obstacle.

3.4 Mean Flow Parameters

The skin friction coefficients (c_f') for all profiles were determined by plotting the mean velocity data on axes u/U_1 versus $\log_{10} y(U_1/\nu)$ and comparing the wall region of the profile with the law of the wall (Equation (1)) expressed in Clauser's[6] form:

$$(u/U_1) = 5{\cdot}76(c_f'/2)^{1/2} \log_{10} y(U_1/\nu) + 5{\cdot}76(c_f'/2)^{1/2} \log_{10} (c_f'/2)^{1/2} + 5{\cdot}1(c_f'/2) \qquad (5)$$

Most profiles showed good agreement with the Clauser lines and hence reliable values of skin friction coefficient could be inferred. Early profiles in the small gap flows did show sinuousity as was discussed with reference to Figure 3 and thus the skin friction coefficients for these profiles were more doubtful.

Ratios of local skin friction coefficient to the skin friction coefficients of an undisturbed layer are plotted in Figure 6 for all gap sizes as a function of distance from the gap. During the distortion phase ($0 < x/H < 10$) different wall shear distributions are produced for flows through different gap sizes. For flow through small gaps ($D/H < 5$) the centreline flow approaches separation under the influence of the gap edge vortices, so that the skin friction coefficients approach zero. For the smallest gap studied ($D/H = 0{\cdot}5$) the flow only just remains attached. As gap size increases, the gap edge separations are moved away from the flow centreline and occupy a smaller proportion of the flow area in the gap; thus the minimum skin friction on the centreline increases. At the largest gap size ($D/H = 10{\cdot}0$) the increased velocity through the gap results in a centreline skin friction coefficient that exceeds the undisturbed value for $x/H < 20$.

During the initial readjustment phase the skin friction distributions depend on the value at the end of the distortion phase. However, all distributions are approaching the final equilibrium value of skin friction from below at the last measuring station. The behaviour of the skin friction distributions at $x/H = 224$ is not however uniform: extrapolated distributions for small gap settings overshoot the equilibrium value a short distance downstream of $x/H < 224$, whereas those for the two largest settings do not.

For the zero gap case Bradshaw and Wong[2] also reported overshooting of the equilibrium skin friction coefficient. Another point of agreement of these results with previous work is the position of reattachment for the zero gap case which, as shown in Figure 6, occurs at approximately $x/H = 8$. This broadly agrees with previous results by Mueller and Robertson[11] (reattachment at $x/H \simeq 7$), Oka and Kostic[12] (at $x/H \simeq 7$) and Counihan *et al.*[5] (at $x/H \simeq 6$).

An accurate mean velocity profile shape factor was introduced by Clauser[6] and is defined as

$$G = \int_0^\delta \left(\frac{U_1 - u}{u_\tau}\right)^2 dy \Big/ \int_0^\delta \left(\frac{U_1 - u}{u_\tau}\right) dy \qquad (6)$$

For an undisturbed zero pressure gradient layer at high Reynolds number, G has a value of about $6{\cdot}8$. Perturbations applied to a zero pressure gradient layer cause G to vary from this equilibrium value. The variation of G after a perturbation is a useful indication of the degree of distortion and subsequent readjustment of the whole layer. Distributions of G for all gap sizes in the present experiment have been plotted in Figure 7. Not surprisingly, maximum distortion (i.e. largest G variation) occurs downstream of the smallest gaps. However, the profile distortion is remarkably similar for all gap sizes after about $x/H = 60$, which reinforces the previous conclusion that layers forget their distortion history in the readjustment region and follow

similar paths back to equilibrium conditions. There are, however, minor differences in G variation at large distances from the gap. Values of G for small gap flows undershoot the equilibrium value at $x/H = 224$ whereas for the largest gaps G approaches the equilibrium value monotonically. Undershooting for the zero gap case has been previously reported by Bradshaw and Wong,[2] who found that the minimum value of G occurred at

$$x/H = 100\sqrt{\delta/H}$$

which for the present experiment gives $x/H = 316$ as the position for minimum G which seems reasonable for the data presented in Figure 7.

3.5 Turbulent Flow

Figure 8 plots the maximum non-dimensional longitudinal turbulent intensity ($\sqrt{\overline{u_m'^2}}/u_{\tau 0}$) for each profile, and the height of this maximum from the wall, as a function of distance from the gap. There are again different behaviours for flow through small and large gaps. Small gaps produce large maximum values of $\sqrt{\overline{u_m'^2}}$ which are attained shortly after the gap and are (approximately) maintained throughout the distortion region. $\sqrt{\overline{u_m'^2}}$ decays from this maximum value in the readjustment region. The graphs are truncated at $x/H = 56$ because flow readjustment produces profiles, downstream of $x/H = 56$, in which $\sqrt{\overline{u_m'^2}}$ reverts to a position very near the wall as in the undisturbed upstream profile (see Fig. 2).

Figure 8 also plots y_m' (the distance from the wall to $\sqrt{\overline{u_m'^2}}$) which is initially constant and then suddenly increases with increasing distance downstream of the gap. This sudden increase commences at progressively larger distances as the gap is increased. For the largest gap ($D/H = 10{\cdot}0$) an increase in y_m' does not occur within the observation range.

These results are consistent with flow mechanisms previously described. Increasing values of y_m' with distance reflect a flow adjustment that works outwards from the wall. High initial values of $\sqrt{\overline{u_m'^2}}$ for small gap flows reflect the higher turbulence levels generated by the gap edge separations. For large gap flows, turbulence is generated at the beginning of, and as part of, the readjustment process. These large gap turbulence profiles thus have a small maximum which appears near the end of distortion or at the beginning of readjustment.

4. CONCLUSIONS

(1) Boundary layer flow through a gap in a small isolated roughness element consists of a flow distortion region followed by a flow readjustment region. The distortion region extends about 10–16 element heights downstream of the element. The following readjustment region appears to extend for several hundred element heights downstream of the element.

(2) Centreline flow through small gaps has, compared with an undisturbed flow:

(i) an increased longitudinal turbulence intensity near the wall;

(ii) a decreased mean velocity near the wall;

(iii) a large decrease in wall shear up to $x/H = 50$; and

(iv) a large change in mean profile shape up to $x/H = 50$.

Conversely, the centreline flow through large gaps has

(i) a decreased longitudinal turbulence intensity near the wall;

(ii) an increased mean velocity in the distortion region; and

(iii) little change in wall shear or in mean profile shape.

(3) The mechanism of flow readjustment downstream of distortion proceeds by a flow modification that works outwards from the wall. Both the fluctuating and mean flow fields are modified; the modification of the fluctuating flow precedes the mean flow modification for all gap sizes. The growth of this new internal layer as a function of distance from the gap can be collapsed (for all six cases) onto a single curve with little scatter if the parameters are non-dimensionalized with the local wall length scale. This

curve is usefully approximated by a relation derived by Townsend for flow over a roughness perturbation.

(4) Initial readjustment of centreline flow parameters (c_f' and G) depends on their values at the end of distortion. However, later readjustment behaviour is similar for all gap sizes with the parameter curves and the mean and fluctuating profiles being similar for $x/H > 100$.

(5) Boundary layer flow over an isolated element without a gap can be regarded as a limiting case of boundary layer flow through a gap. In the zero gap case, profile shapes and parameter variations downstream of reattachment follow the pattern set by centreline flows through small gaps.

REFERENCES

1. Antonia, R. A., and Luxton, R. E. (1972). "The Response of a Turbulent Boundary Layer to a Step Change in Surface Roughness—Part 2: Rough-to-Smooth." *J. Fluid Mech.* **53**, 737.

2. Bradshaw, P., and Wong, F. Y. F. (1972). "The Reattachment and Relaxation of a Turbulent Shear Layer." *J. Fluid Mech.* **52**, 113.

3. Brown, K. C. (1971). *Three-Dimensional Turbulent Boundary Layers.* Ph.D. Thesis, University of Melbourne.

4. Castro, I. P., and Robins, A. G. (1977). "The Flow Around a Surface-Mounted Cube in Uniform and Turbulent Streams." *J. Fluid Mech.* **79**, 307.

5. Counihan, J., Hunt, J. C. R., and Jackson, P. S. (1974). "Wakes Behind Two-Dimensional Surface Obstacles in Turbulent Boundary Layers." *J. Fluid Mech.* **64**, 529.

6. Clauser, F. H. (1954). "Turbulent Boundary Layers in Adverse Pressure Gradients." *J. Aeronautical Sci.* **21**, 91.

7. Clauser, F. H. "The Turbulent Boundary Layer." *Advances in Applied Mech.*, Vol. IV, pp. 1-51.

8. Good, M. C., and Joubert, P. N. (1968). "The Form Drag of Two-Dimensional Bluff Plates Immersed in Turbulent Boundary Layers." *J. Fluid Mech.* **31**, 547.

9. Hornung, H. G., and Joubert, P. N. (1963). "The Mean Velocity Profile in Three-Dimensional Turbulent Boundary Layers." *J. Fluid Mech.* **15**, 368.

10. Klebanoff, P. S., and Diehl, Z. W. (1951). *Some Features of Artificially Thickened Fully Developed Turbulent Boundary Layers with Zero Pressure Gradient.* NACA, TN 2475.

11. Mueller, T. J., and Robertson, M. R. (1962). *A Study of the Mean Motion and Turbulence Downstream of a Roughness Element.* Proc. First Southeastern Conf. on Theoretical and Applied Mechanics, pp. 326-340.

12. Oka, S., and Kostic, Z. (1972). *Influence of Wall Proximity on Hot Wire Velocity Measurements.* DISA Information No. 13, pp. 29-33.

13. Petryk, S., and Brundrett, E. (1967). *Recovery of a Turbulent Boundary Layer Disturbed by a Single Roughness Element.* Res. Rept. No. 4, Dept. of Mech. Eng., Univ. of Waterloo.

14. Phataraphruk, P., and Logan, E. (1978). *Response of a Turbulent Pipe Flow to a Single Roughness Element.* Proc. Ninth Southeastern Conf. on Theoretical and Applied Mechanics, pp. 139-49.

15. Sami, S., and Liu, W. H. (1978). *Confined Shear Layer Approaching a Stagnation Point.* Proc. Fourteenth Midwestern Mech. Conf. Developments in Mechanics, Vol. 8, pp. 497-516.

16. Schofield, W. H. (1973). *The Effect of Sudden Discontinuities on Turbulent Boundary Layer Development.* ARL/ME Report 139.

17. Schofield, W. H. (1977). *The Response of Turbulent Shear Flows to Discontinuous Changes in Surface Roughness.* ARL/ME Report 150.

18. Schofield, W. H. (1975). "Measurements in Adverse-Pressure-Gradient Turbulent Boundary Layers with a Step Change in Surface Roughness." *J. Fluid Mech.* **70**, 573.

19. Sharan, V. K. (1975). "On Characteristics of Flow Around Building Models with a View to Simulate the Minimum Fraction of the Natural Boundary Layer." *Intl. J. Mech. Sci.* **17**, 557.

20. Tani, I. (1969). *Review of Some Experimental Results of the Response of a Turbulent Boundary Layer to Sudden Perturbations.* AFSOR-IFP-Stanford Conference, Vol 1, pp. 483–94.

21. Townsend, A. A. (1976). *Structure of Turbulent Shear Flow*, 2nd Ed., pp. 308–13, C.U.P.

22. Wieghardt, K., and Tillman, W. (1951). *On the Turbulent Friction Layer for Rising Pressure.* NACA, TM 1314.

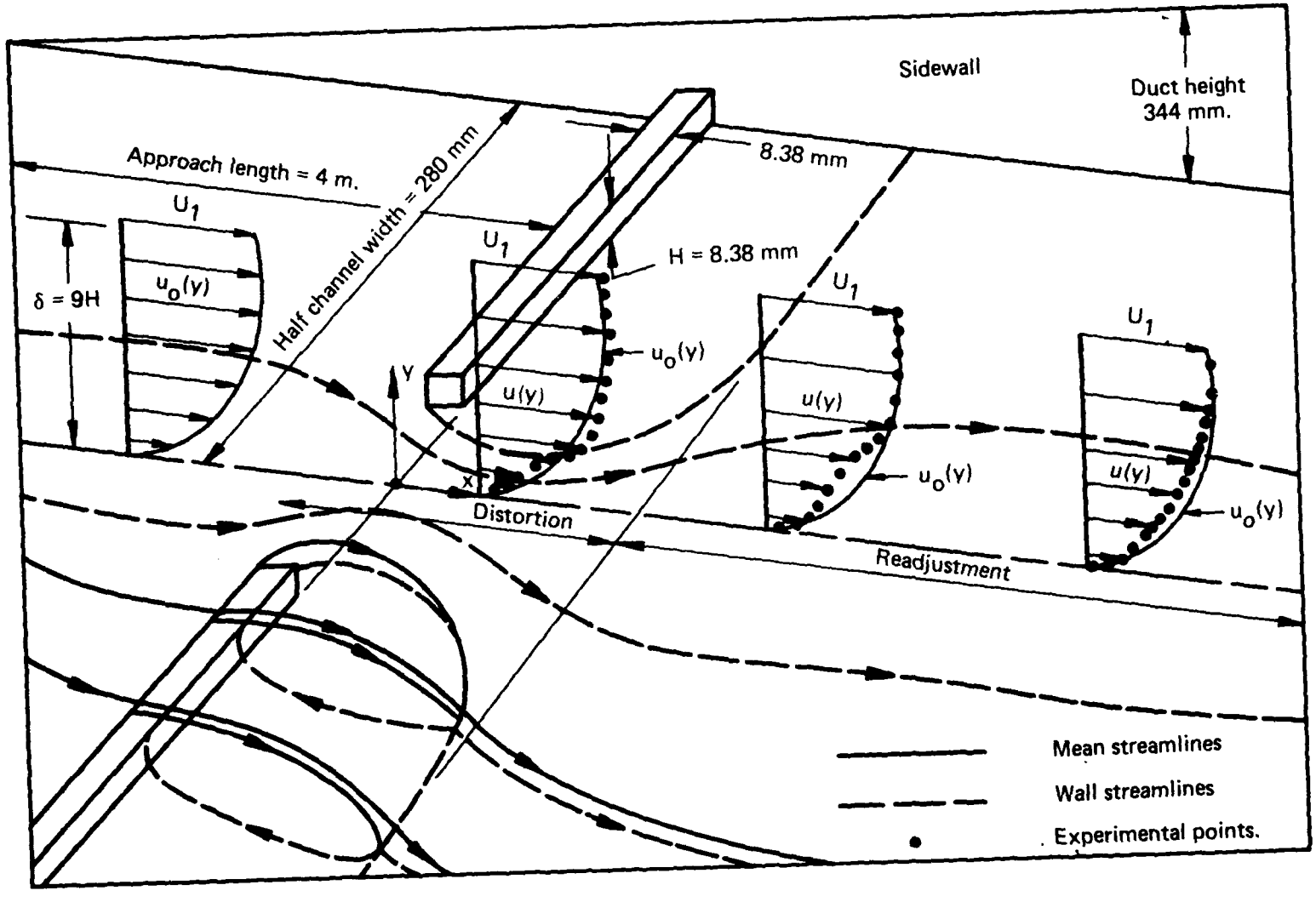

FIG. 1 SCHEMATIC VIEW OF EXPERIMENTAL FLOW

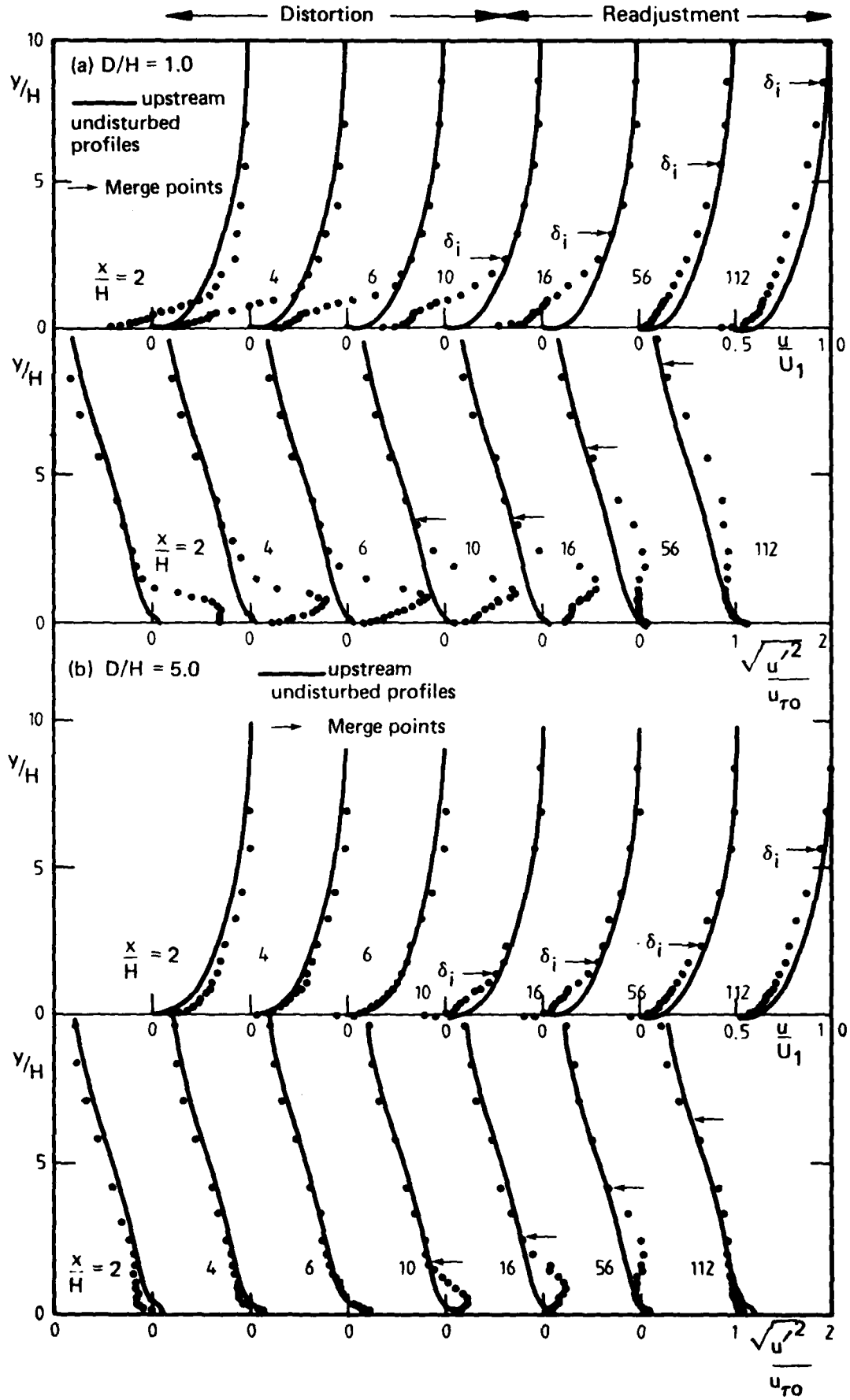

FIG. 2 SELECTED MEAN VELOCITY AND LONGITUDINAL TURBULENCE INTENSITY

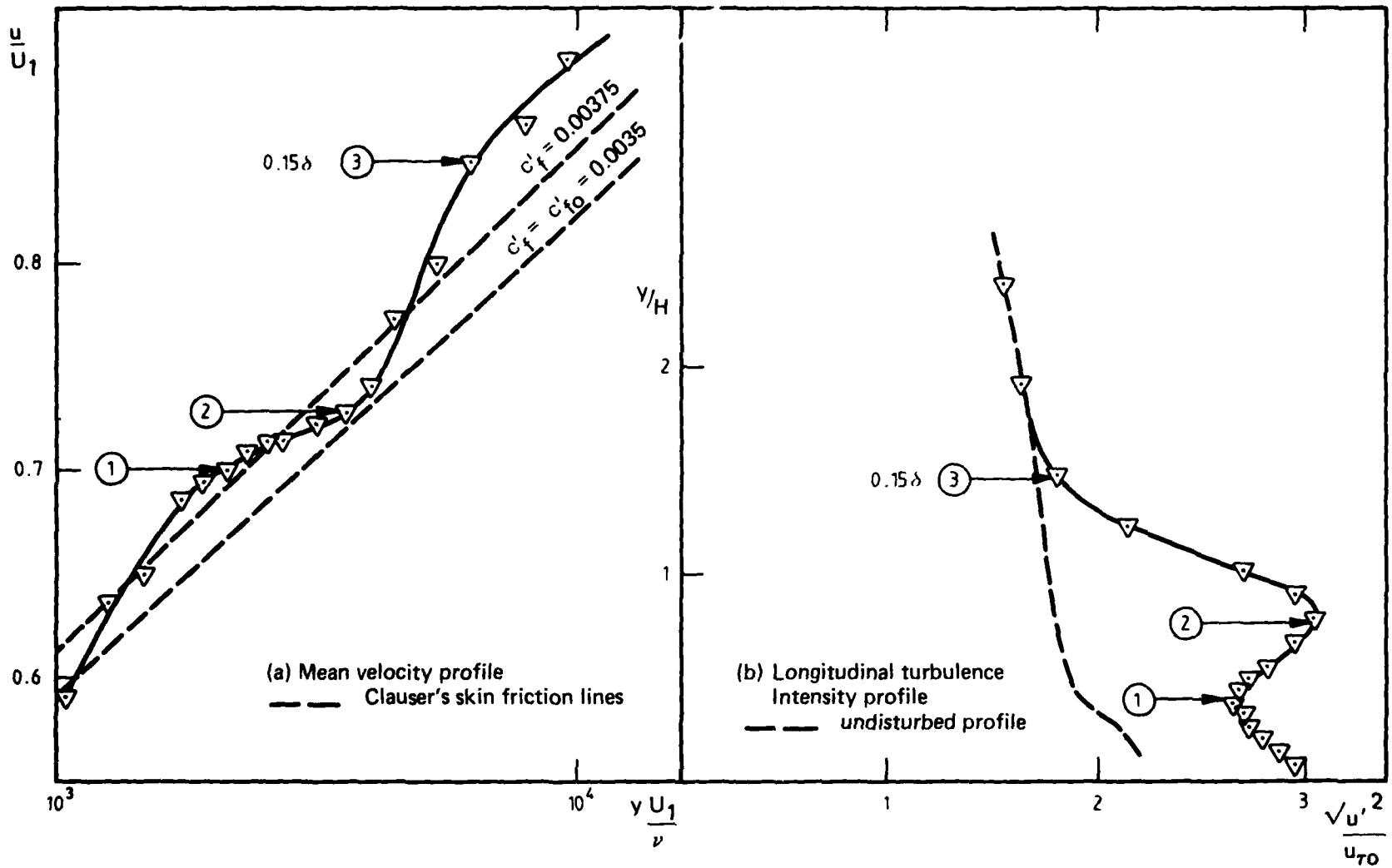

FIG. 3 MEAN VELOCITY AND LONGITUDINAL TURBULENCE INTENSITY PROFILES FOR D/H = 0.5 at x/H = 0

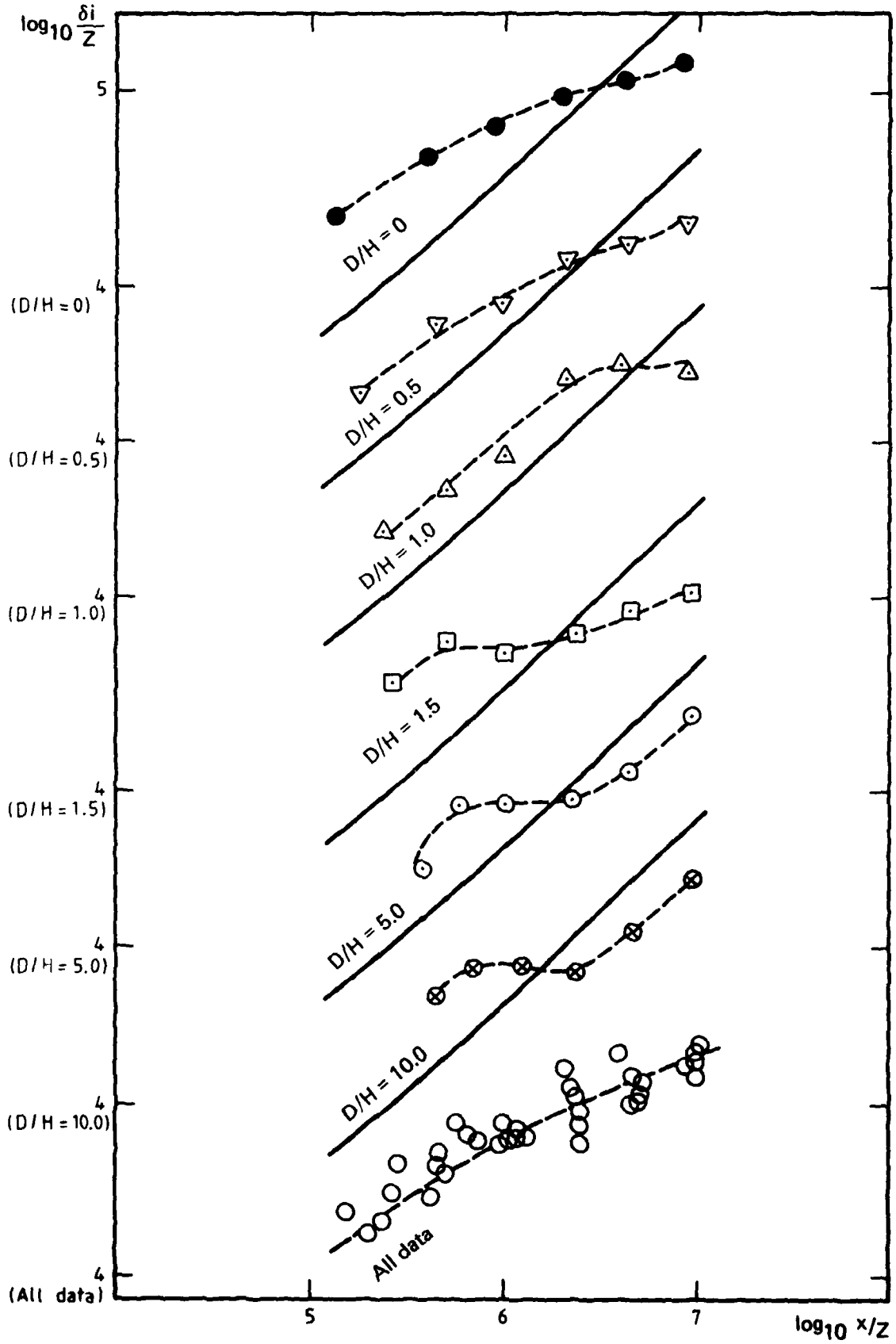

—— equation 4; – – mean line.

FIG. 4 INTERNAL LAYER GROWTH

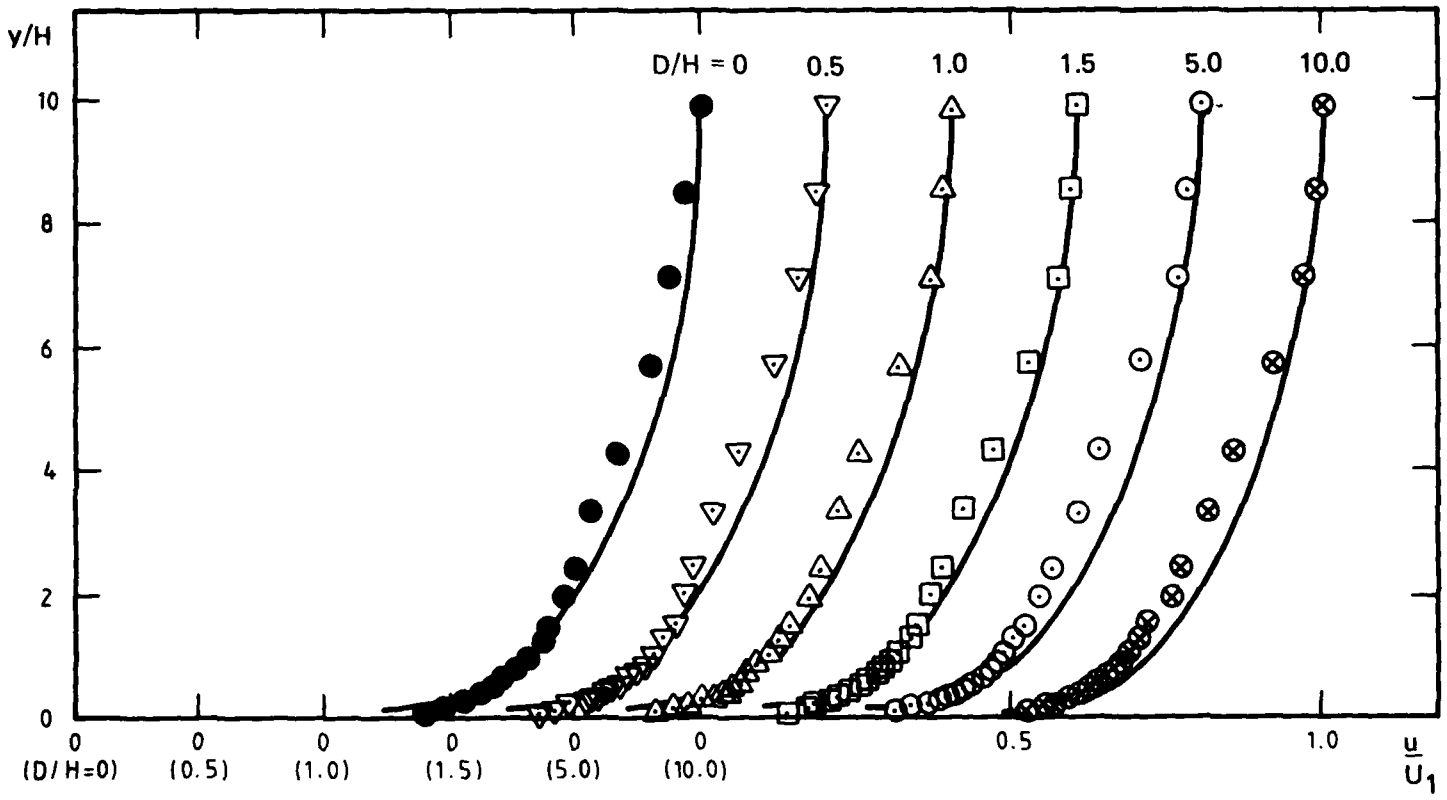

FIG. 5 MEAN VELOCITY AND LONGITUDINAL TURBULENCE PROFILES AT x/H = 224 FOR ALL GAP SIZES

(a) Mean velocity profiles at x/H = 224

——— , undisturbed profile

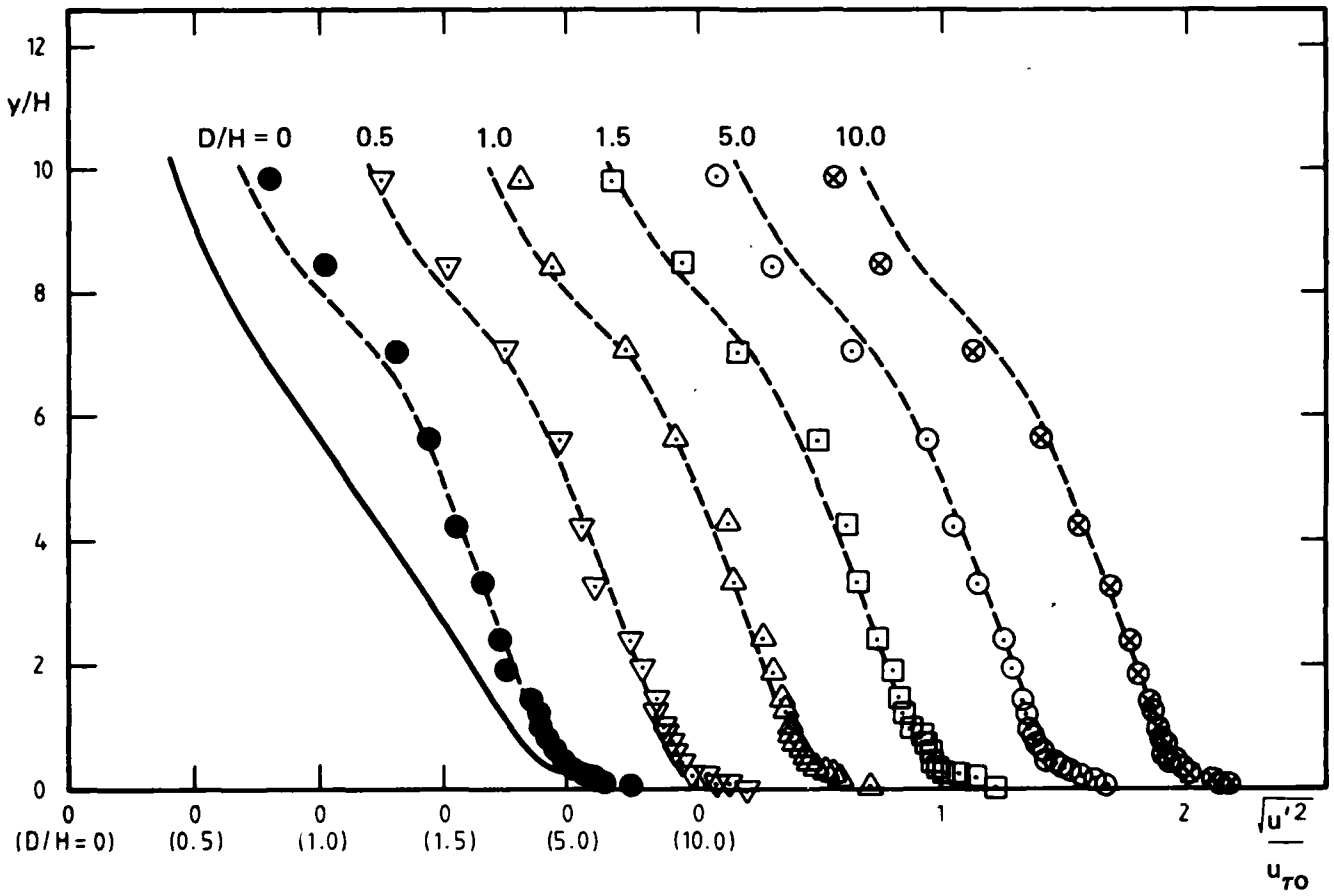

FIG. 5 MEAN VELOCITY AND LONGITUDINAL TURBULENCE PROFILES AT x/H = 224 FOR ALL GAP SIZES

(b) Longitudinal turbulence intensity profiles at $\frac{x}{H}$ = 224.

——— undisturbed profile

– – – mean profile at x/H = 224.

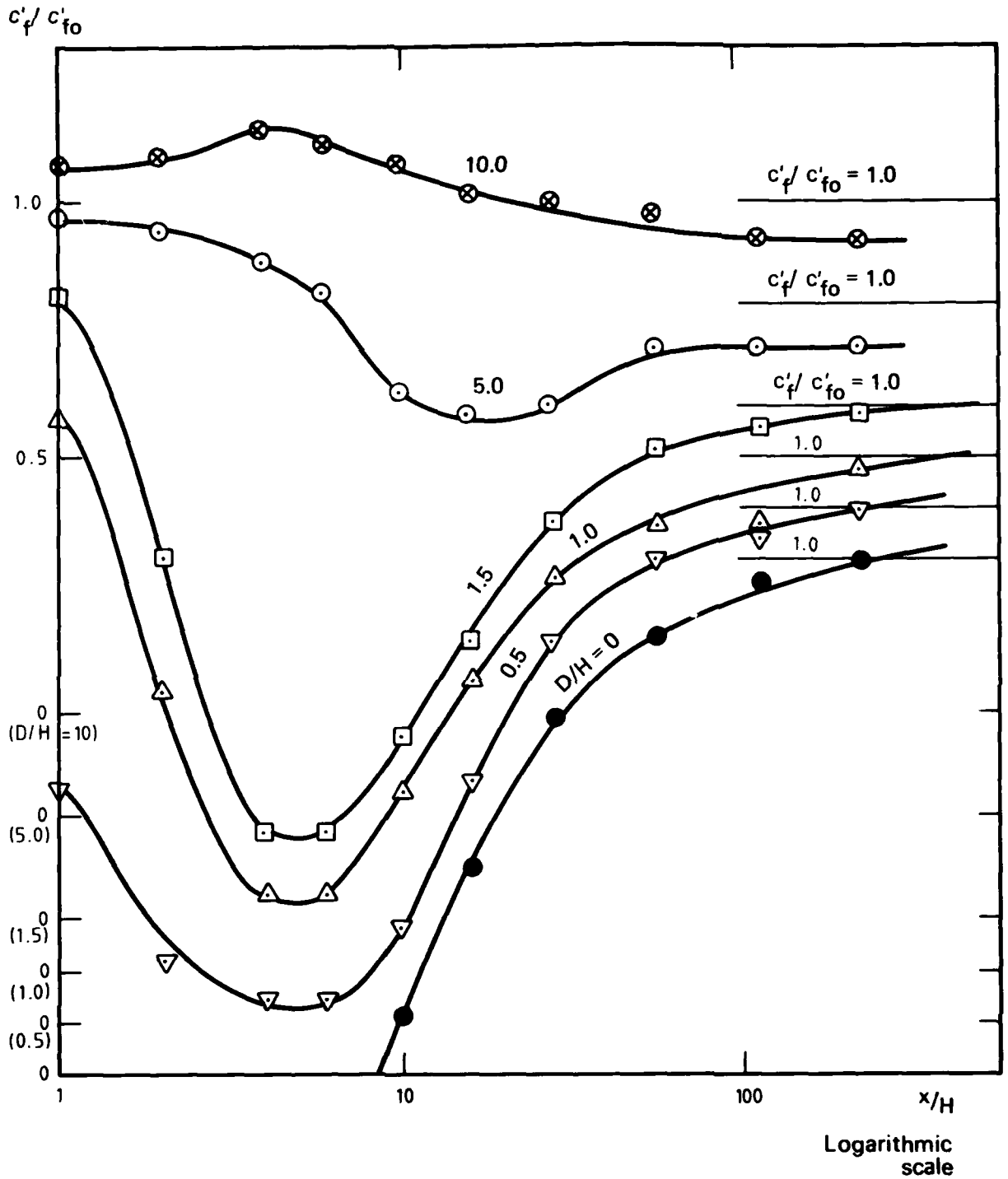

FIG. 6 SKIN FRICTION COEFFICIENTS

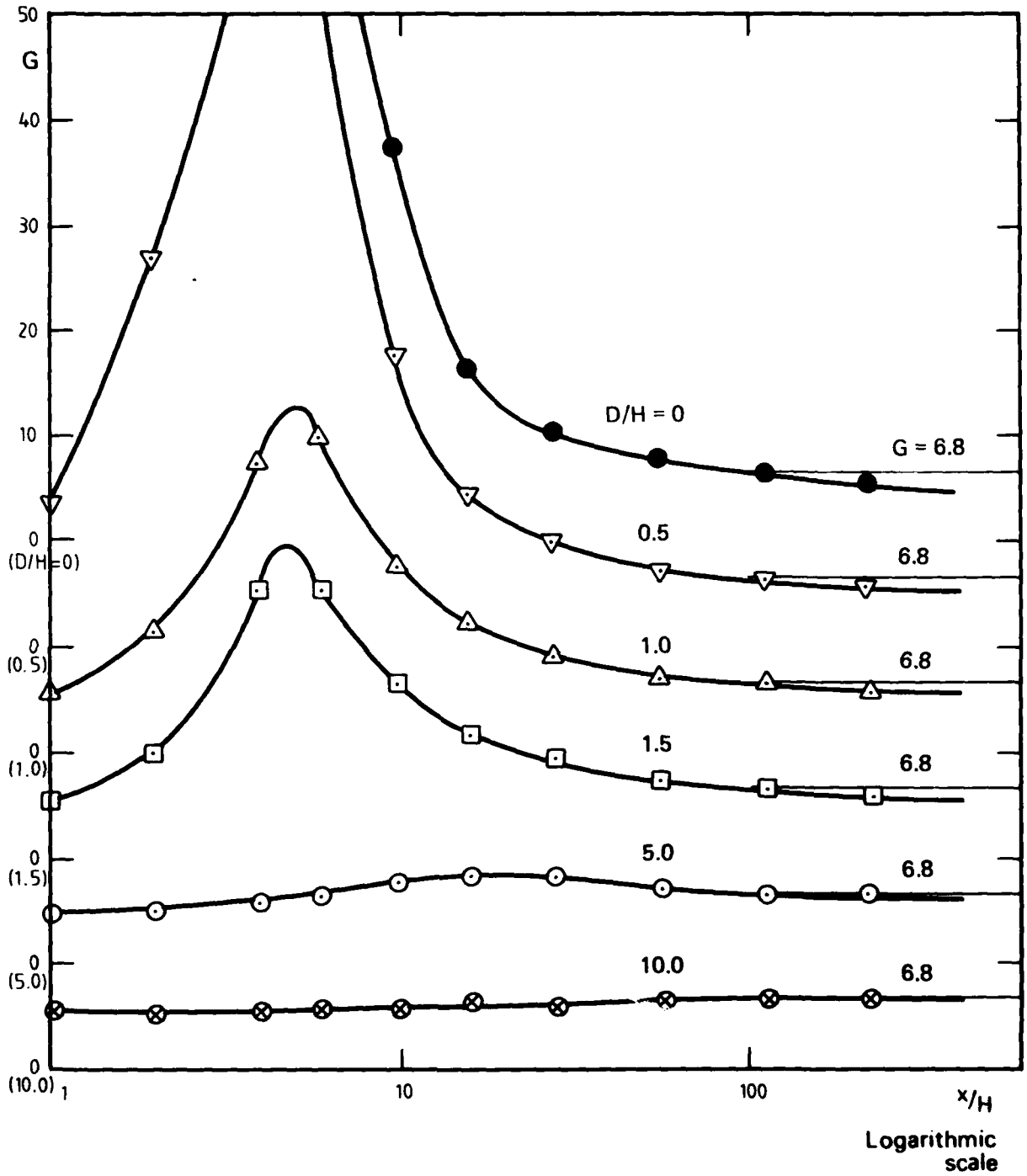

FIG. 7 CLAUSER'S MEAN PROFILE SHAPE PARAMETER

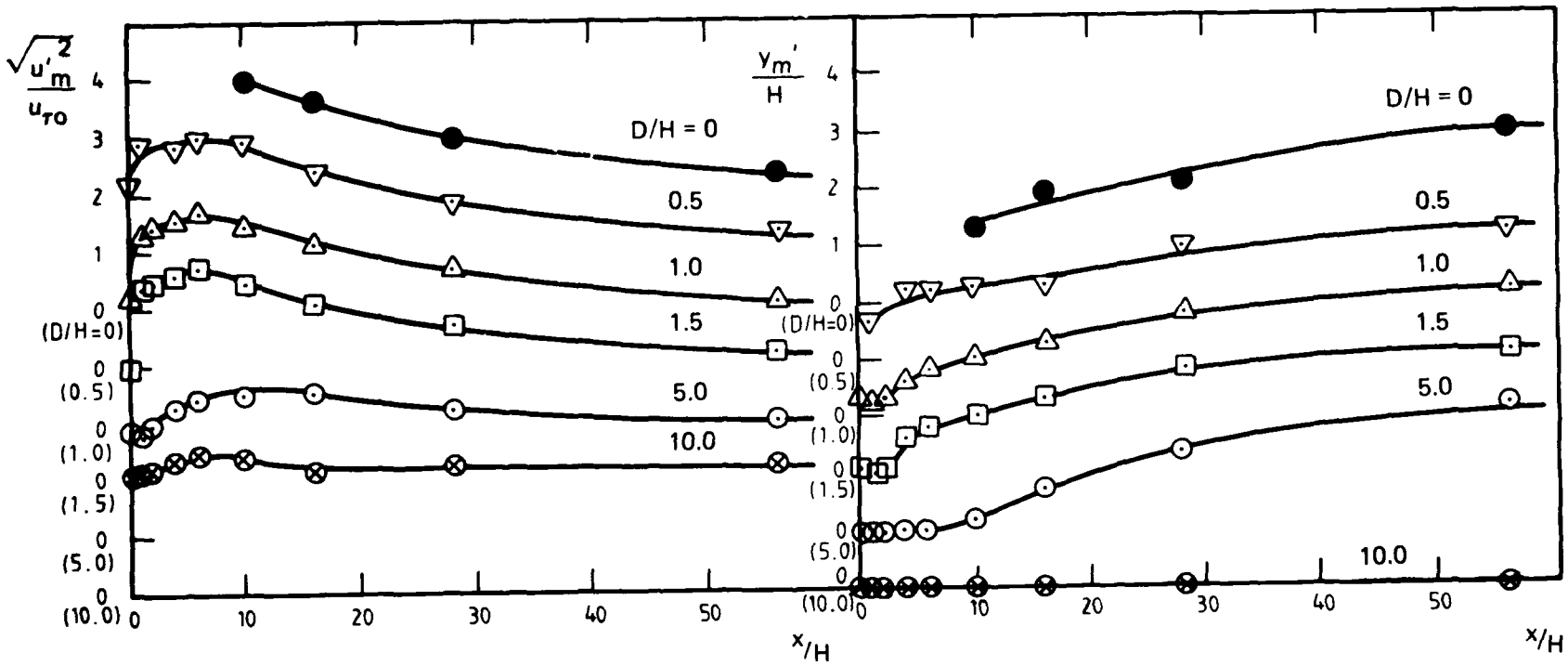

FIG. 8 MAXIMUM VALUES OF LONGITUDINAL TURBULENCE INTENSITY AND DISTANCE FROM WALL OF THESE MAXIMA

DISTRIBUTION

	Copy No.
AUSTRALIA	
Department of Defence	
Central Office	
Chief Defence Scientist	1
Deputy Chief Defence Scientist	2
Superintendent, Science and Technology Programs	3
Australian Defence Scientific and Technical Representative (UK)	—
Counsellor, Defence Science (USA)	—
Defence Library	4
Joint Intelligence Organisation	5
Document Exchange Centre, DISB	6–23
DGAD (NCO)	24–27
Aeronautical Research Laboratories	
Chief Superintendent	28
Library	29
Superintendent – Mechanical Engineering Division	30
Divisional File—Mechanical Engineering	31
Authors: W. H. Schofield	32–36
D. S. Barber (USA)	37–38
E. Logan (USA)	39–40
Materials Research Laboratories	
Library	41
Defence Research Centre, Salisbury	
Library	42
Central Studies Establishment	
Information Centre	43
Engineering Development Establishment	
Library	44
RAN Research Laboratory	
Library	45
Mr. I. F. P. Jones	46
Dr. P. Mulhearn	47
Navy Office	
Naval Scientific Adviser	48
Army Office	
Army Scientific Adviser	49
Royal Military College, Library	50
Air Force Office	
Aircraft Research and Development Unit, Scientific Flight Group	51
Air Force Scientific Adviser	52
Technical Division Library	53
DGAIRENG--AF	54
HQ Support Command (SENGSO)	55

Department of Productivity

Government Aircraft Factories

Manager		56
Library		57

Statutory, State Authorities and Industry

Australian Atomic Energy Commission, Director		58
CSIRO, Mechanical Engineering Division, Chief		59
SEC of Victoria, Herman Research Laboratory, Librarian		60
Commonwealth Aircraft Corporation, Library		61
Hawker de Havilland Pty. Ltd.		
Librarian, Bankstown		62
Manager, Lidcombe		63

Universities and Colleges

Adelaide	Professor of Mechanical Engineering	64
	Prof. R. E. Luxton	65
Melbourne	Engineering Library	66
	Prof. P. N. Joubert	67
	Dr. A. E. Perry	68
Newcastle	Prof. R. A. Antonia	69
Sydney	Engineering Library	70
	Prof. G. A. Bird	71
	Prof. R. I. Tanner	72
	Prof. R. Bilger	73
New South Wales	Prof. R. A. A. Bryant	74
Queensland	Prof. K. Bullock	75
Tasmania	Prof. A. R. Oliver	76
	Dr. G. Walker	77
RMIT	Library	78

CANADA

National Aeronautical Establishment, Library	79
Division of Mechanical Engineering, Director	80
Gas Dynamics Laboratory, Mr. R. A. Tyler	81
Toronto University, Institute for Aerospace Studies	82

FRANCE

AGARD, Library	83
ONERA, Library	84
Service de Documentation, Technique de l'Aeronautique	85

GERMANY

Ruhr-Universitat, Bochum—Institut fur Thermo- und Fluiddynamik (Dr Miyata)	86

INDIA

Defence Ministry, Aero. Development Establishment, Library	87
Hindustan Aeronautics Ltd., Library	88
Indian Institute of Science, Library	89
Indian Institute of Technology, Library	90
National Aeronautical Laboratory, Director	91

ISRAEL

Technion – Israel Institute of Technology, Prof. J. Singer	92

ITALY

Associazione Italiana di Aeronautica e Astronautica	93

JAPAN

National Aerospace Laboratory, Library	94
Tokyo University, Inst. of Space and Aeroscience	95

NETHERLANDS

National Aerospace Laboratory (NLR), Library	96
Eindhoven Univ. of Technology, Dept. of Applied Physics (Dr. Koppius)	97

NEW ZEALAND

Canterbury University	
Mr. F. Fahy, Mechanical Engineering	98
Prof. D. Stevenson, Mechanical Engineering	99

SWEDEN

Aeronautical Research Institute	100
SAAB-Scania, Library	101

SWITZERLAND

Institute of Aerodynamics, Prof. J. Ackeret	102

UNITED KINGDOM

Aeronautical Research Council, Secretary	103
CAARC, Secretary	104
Royal Aircraft Establishment	
Farnborough, Library	105
Mr. L. F. East	106
National Gas Turbine Establishment, Director	107
National Physical Laboratories, Library	108
British Library, Science Reference Library	109
Aircraft Research Association, Library	110
Rolls-Royce (1971) Ltd.	
Aeronautics Division, Chief Librarian	111
Bristol Siddeley Division, T. R. & I. Library Services	112
Ruston & Hornsby, Turbine Division, Mr. A. V. Jackman	113
British Aerospace Corporation, Aircraft Group	
Kingston-upon-Thames, Headquarters Library	114
Manchester Division	115
British Hovercraft Corporation Ltd., Library	116
Westland Helicopters Ltd.	117

Universities and Colleges

Bristol	Prof. L. Howarth, Engineering Dept.	118
Cambridge	Sir William Hawthorne, Engineering Dept.	119
London	Prof. A. D. Young, Aero. Engineering	120
Belfast	Dr. A. Q. Chapleo, Aero. Engineering	121
Manchester	Prof. N. Johannessen, Fluid Mechanics	122
Cranfield Institute of Technology	Prof. Lefebvre	123
Imperial College	Prof. of Mechanical Engineering	124
	Prof. B. G. Neal, Struct. Engineering	125
	Prof. P. Bradshaw	126
	Dr. D. H. Wood	127

UNITED STATES OF AMERICA

NASA Scientific and Technical Information Facility	128
Sandia Group Research Organisation	129
American Institute of Aeronautics and Astronautics	130
Applied Mechanics Review	131

Bell Helicopter Textron		132
Boeing Co., Head Office, Mr. R. Watson		133
General Electric, Aircraft Engine Group		134
Lockheed Missiles and Space Company		135
McDonnell Douglas Corporation, Director		136
Calspan Corporation		137
United Technologies Corporation		
Fluid Dynamics Laboratories		138
Pratt & Whitney Aircraft Group		139
Universities and Colleges		
Arizona State	Prof. D. Metzger	140
	Prof. N. Berman	141
Florida	Aero. Engineering Dept.	142
Harvard	Prof. G. F. Carrier, Applied Maths	143
	Dr. S. Goldstein	144
Johns Hopkins	Prof. S. Corrsin	145
Iowa State	Dr. G. K. Serory, Mechanical Eng.	146
Princeton	Prof. G. L. Mellor, Mechanics	147
Stanford	Department of Aeronautics, Library	148
California Institute of Technology	Guggenheim Aeronautical Labs., Library	149
Massachusetts Institute of Technology	Library	150
Southern Methodist University, Texas	School of Engineering and Applied Sciences (Prof. R. L. Simpson)	151
Spares		152-157